ACS OMEGA

Open Access

This article is licensed under CC-BY-NC-ND 4.0

http://pubs.acs.org/journal/acsodf

Article

Desorption of Polycyclic Aromatic Hydrocarbons from Microplastics in Human Gastrointestinal Fluid Simulants—Implications for Exposure Assessment

Emeka Ephraim Emecheta, Patrizia Marie Pfohl, Wendel Wohlleben, Andrea Haase,* and Alexander Roloff*

Cite This: *ACS Omega* 2024, 9, 24281−24290

Read Online

ACCESS | Metrics & More | Article Recommendations | Supporting Information

ABSTRACT: Microplastics have been detected in various food types, suggesting inevitable human exposure. A major fraction may originate from aerial deposition and could be contaminated by ubiquitous pollutants such as polycyclic aromatic hydrocarbons (PAHs). While data on the sorption of pollutants to microplastics are abundant, the subsequent desorption in the gastrointestinal tract (GIT) is less understood. This prompted us to systematically investigate the release of microplastics-sorbed PAHs at realistic loadings (44−95 ng/mg) utilizing a physiology-based in vitro model comprising digestion in simulated saliva, gastric, and small and large intestinal fluids. Using benzo[*a*]pyrene as a representative PAH, desorption from different microplastics based on low density polyethylene (LDPE), thermoplastic polyurethanes (TPUs), and polyamides (PAs) was investigated consecutively in all four GIT fluid simulants. The cumulative relative desorption (CRD) of benzo[*a*]pyrene was negligible in saliva simulant but increased from gastric (4 ± 1% − 15 ± 4%) to large intestinal fluid simulant (21 ± 1% − 29 ± 6%), depending on the polymer type. CRDs were comparable for ten different microplastics in the small intestinal fluid simulant, except for a polydisperse PA-6 variant (1−10 μm), which showed an exceptionally high release (51 ± 8%). Nevertheless, the estimated contribution of microplastics-sorbed PAHs to total human PAH dietary intake was very low (≤0.1%). Our study provides a systematic data set on the desorption of PAHs from microplastics in GIT fluid simulants.

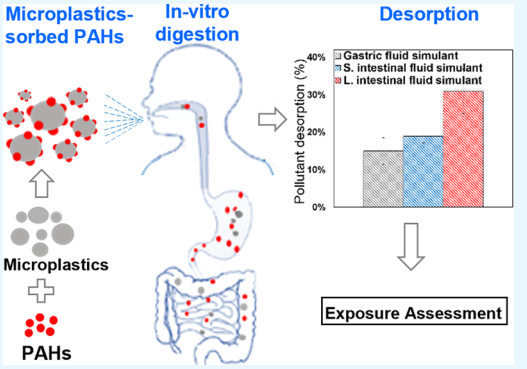

1. INTRODUCTION

As a result of the continuous increase in plastic production, mismanaged plastic waste has commensurably increased to emerge as a global health concern.[1,2] At the present growth rate in production, plastic waste is projected to triple from the current estimate of 99 metric tonnes per year within the next 40 years.[3] In the environment, larger plastic debris degrades and fragments into smaller particles including micro- and nanoplastics (MNPs), which are already ubiquitous.[2,4]

MNPs also have been frequently detected in several beverages and food products such as tap and bottled water,[5] fruits and vegetables,[6] milk,[7] beer and soft drinks,[8,9] salt,[10] and different kinds of fish and fishmeal.[11] These widespread occurrences of MNPs in our ecosystem have made human exposure inevitable. Evidence of MNPs in feces[12,13] confirms human consumption and subsequent passage through the gastrointestinal tract (GIT). In addition, high concentrations of different MNP particles have been reported in certain indoor and outdoor air settings.[14,15] In particular, the detection of MNPs in human lung tissues confirms human inhalation exposure.[16] Notably, the majority of directly inhaled MNPs may subsequently be swallowed into the GIT following mucociliary clearance from the respiratory tract.[17−19] Additionally, a significant fraction of the MNPs present in food is estimated to be deposited from indoor air.[20,21] However, while these reports have generated concerns about the effects of MNPs on human health,[19] a direct adverse health effect remains subject to controversy and uncertainty.[22,23]

It has been speculated that MNP particles might act as carriers for environmental contaminants such as persistent organic pollutants (POPs). Similar to MNPs, many POPs are ubiquitous.[24] For example, sorption of polycyclic aromatic hydrocarbons (PAHs) to MNPs collected from the environment has been demonstrated.[25−27] Therefore, it is conceivable that MNPs entering the GIT via food, water and dust could potentially contain sorbed environmental pollutants.[28] Some of

Received: November 24, 2023
Revised: April 16, 2024
Accepted: April 19, 2024
Published: May 24, 2024

© 2024 The Authors. Published by American Chemical Society

these microplastic-sorbed pollutants are highly toxic and are known for their carcinogenic,[29] mutagenic,[29] immunotoxic,[30] inflammatory, or endocrine-disruptive effects.[31] In the GIT, desorption of POPs, including PAHs, from ingested MNPs could contribute to aggregate human exposure to chemicals.

Several studies have investigated the release of microplastic-sorbed organic pollutants in marine organisms and birds using artificial gut fluids or model simulations.[32−35] Here, we focus on the potential release of MNP-sorbed PAHs in the human GIT as a continuation of our previous work,[36] where we systematically investigated the sorption of PAHs to MNPs. Among the studied particles were intentionally produced MNPs used in additive manufacturing applications. These include variants of polyamide (PA-6) and thermoplastic polyurethane (TPU), as well as cross-linked PU and PA-12, which feature growing utilization in commercial 3D-printing. For comparison, MNPs derived from polymers commonly used for packaging and production materials such as low-density polyethylene (LDPE), poly(methyl methacrylate) (PMMA), as well as cryomilled end-of-life truck tire tread were also investigated.

To provide realistic insight into the fate of MNP-sorbed PAHs in the human GIT, a physiology-based in vitro digestion model anchored on the DIN 19738 standard was modified to sequentially simulate the release of PAHs from MNPs in the saliva, gastric, small, and large intestine fluids. Therefore, 11 different MNPs and five photoaged MNP variants were loaded with benzo[*a*]pyrene (B[*a*]P). As PAHs often occur as variable mixtures, B[*a*]P is sometimes considered representative for other PAHs owing to its ubiquity and well-characterized toxicity.[29] For comparison, anthracene (Anth) and dibenzo-[*a,l*]pyrene (DB[*a,l*]P) were also investigated for selected MNPs. Notably, unlike most studies on the desorption behavior of microplastics,[35,38,39] our work focuses on polydisperse MNPs with environmentally relevant size distributions, that have been produced from larger particles through cryomilling deploying different sieve sizes. The resulting particles feature polymer compositions, morphologies, and size ranges considered to be realistic for secondary MNPs.

Moreover, efforts were made to estimate the extent to which MNPs contribute to the overall intake of PAHs in the human diet. While it has been suggested that the contribution via marine organisms is negligible,[34,37] the contribution of MNPs to PAH intake in humans has been either estimated through probabilistic modeling or remains undisclosed in the limited studies that have examined PAH desorption from MNPs.[38,39] Concerned by this paucity of data, the Food and Agriculture Organization of the United Nations (FAO) and the World Health Organization (WHO) recently estimated the significance of microplastics to human PAH exposure using contaminated fish and drinking water as models, albeit assuming complete desorption of PAHs in the GIT.[23,40]

To the best of our knowledge, this is the first systematic study on the in vitro release of MNP-sorbed PAHs in all four human gastrointestinal compartments, which also provides an estimate on the exposure to bioaccessible PAHs via MNP intakes based on measured release rates.

2. MATERIALS AND METHODS

2.1. Materials and Chemicals. The MNPs from different suppliers (see Table S1 for details) were cryomilled as described in our previous study,[41] and therefore varied in size and shape as confirmed by scanning electron microscopy (SEM) imaging (see the Supporting Information (SI), Figure S1). In total, 11 MNP variants from six polymer classes were investigated. Among them are additive manufacturing-relevant polymers such as polyamides (PA-12_44, PA-6_42, PA-6_7), polyurethane (PU_1C_arom), and thermoplastic polyurethanes (TPUs). The TPUs[42] consist of soft and hard segments. The soft segments comprise polyester or polyether polyols (termed 'ester' or 'ether'), while the hard segments are built from aromatic or aliphatic diisocyanates (termed 'arom' or 'alip'). For comparison, low-density polyethylene (LDPE), poly(methyl methacrylate) (PMMA), and Tire Rubber particles were also studied.

The size distributions of the investigated MNPs are reported in the SI (Section S1). Other physicochemical properties of the MNP materials have been described in our previous study.[36] To investigate the effect of photoaging on the desorption behavior of the additive manufacturing-relevant MNPs, selected MNP variants (PA-6_42, TPU_ester_arom and TPU_ether_arom) were artificially aged via exposure to ultraviolet (UV) light for 1000 and 2000 h following a procedure described previously.[43]

Anth, B[*a*]P, DB[*a,l*]P (Table S2), anthracene-d_{10} (Anth-d_{10}), benzo[*a*]pyrene-d_{12} (B[*a*]P-d_{12}), and dibenzo[*a,i*]pyrene (DB[*a,i*]P) were purchased as analytical standards in acetonitrile (purity ≥98.5%) from Neochema (Bodenheim, Germany). Hexane (≥99% pure), hydrochloric acid (30% *w*/*v*), and sodium hydroxide pellets (reagent grade) were purchased from Merck (Darmstadt, Germany). Anhydrous magnesium sulfate (99.5%), xylenes (99.0%) and formic acid (≥88% *w*/*v*) were purchased from Sigma-Aldrich (Steinheim, Germany). All components of the gastrointestinal fluid simulants were purchased from Sigma-Aldrich (Steinheim, Germany) in the highest available purity. Ultrapure water was obtained from a Millipore Q-POD dispenser connected to a Millipore milli-Q system (Darmstadt, Germany). All filtrations were performed using 0.7 μm Whatman GF/F Glass Microfiber filters.

2.2. Loading of PAHs onto MNPs. Before in vitro digestion experiments, the MNPs were loaded with Anth, B[*a*]P or DB[*a,l*]P using a batch-equilibrium method similar to that described in our previous work.[36] Briefly, 25 mg MNPs were introduced into a Duran glass vial of 1 L approximate volume (Mainz, Germany). Thereafter, 1.1 L water were introduced into the vial using a Duran glass measuring cylinder (Mainz, Germany) followed by the addition of either 2 μg Anth, B[*a*]P or DB[*a,l*]P from the stock solutions. To achieve a high loading of DB[*a,l*]P on PA-6_42 particles, 25 mg of the polymer was weighted into a glass vial containing 50 mL water and 10 μg DB[*a,l*]P. The mixtures were then incubated on a magnetic stirring plate operated at 600 rotations per minute (rpm) for 6 days at room temperature. After incubation, the PAH-loaded MNPs were separated by filtration and dried overnight inside a gas chromatography oven (Agilent, Waldbronn, Germany) operated at 40 °C. The amount of PAH loaded onto the MNPs, n_{MNP}, was determined indirectly from the amount in the aqueous phase, n_w, by assuming mass balance of the system (eq 1) according to

$$n_{MNP}(\text{ng}) = n_{tot}(\text{ng}) - n_w(\text{ng}) \quad (1)$$

where n_{tot} is the initial total amount of PAH spiked into the vial. n_w was determined by solvent extraction of the filtrate with 2 × 100 mL hexane (see Section S2), and subsequent analysis

https://doi.org/10.1021/acsomega.3c09380
ACS Omega 2024, 9, 24281−24290

Table 1. PAH Loads of MNPs Investigated in This Study (n = 2, Mean ± 2 SD)[a]

		PAH concentrations on MNPs (ng/mg)		
PAHs	MNPs	by mass balance (extraction of the aqueous phase)	calculated from $K_{MNP/w}$	by MNP dissolution and solvent-extraction
B[a]P	PA-6_7	79.1 ± 1.4	79.8 ± 0.2	82.8 ± 3.4
	PA-6_42	79.5 ± 1.0	79.5 ± 0.2	81.2 ± 0.2
	PA-12_44	79.4 ± 0.2	79.4 ± 0.2	_
	LDPE_84	79.1 ± 0.4	79.1 ± 0.2	75.8 ± 44.4
	Tire Rubber	78.8 ± 0.4	78.2 ± 0.4	_
	PMMA_6	61.3 ± 0.6	63.8 ± 6.8	_
	PU_1C_arom	70.3 ± 0.6	71.4 ± 4.8	_
	TPU_est arom	79.0 ± 0.2	75.8 ± 0.6	75.4 ± 8.0
	TPU_est alip	79.3 ± 0.2	77.2 ± 0.6	75.4 ± 8.2
	TPU_eth arom	79.3 ± 0.2	76.7 ± 0.8	84.2 ± 22.4
	TPU_eth alip	79.3 ± 0.4	77.4 ± 1.0	77.3 ± 2.0
Anth	LDPE_84	46.0 ± 16.4	50.2 ± 13.0	_
	PA-6_42	43.5 ± 2.6	55.7 ± 10.2	_
DB[a,l]P	LDPE_84	_	_	52.4 ± 13.8
	PA-6_42	_	_	95.1 ± 7.2

[a]Anth and B[a]P concentrations on MNPs were calculated by mass balance using the measured aqueous concentrations after loading. DB[a,l]P loads were determined by direct extraction of the loaded MNPs. The loadings are comparable to values determined via pre-determined partition coefficients $K_{MNP/w}$[36] as well as direct extraction of selected MNPs. PAH loads on MNPs are within the range of total PAH concentrations in the environment.[44].

of the resulting extract by gas chromatography coupled to mass spectrometry (GC-MS, see Section S4).

For verification, the equilibrium distribution coefficients $K_{MNP/w}$ (eq 2) obtained from previously measured sorption isotherms for PAHs and MNPs[36] were utilized to calculate the expected value for n_{MNP}:

$$K_{MNP/w}(\mathrm{L/kg}) = \frac{n_{MNP}(\mu\mathrm{g})/M_{MNP}(\mathrm{kg})}{n_w(\mu\mathrm{g})/V_w(\mathrm{L})} \quad (2)$$

where M_{MNP} and V_w are the mass of MNPs and volume of water, respectively. As shown in Table 1, both methods yield comparable values for n_{MNP}.

Unlike for Anth and B[a]P, which partition mainly between the water and MNP phases upon equilibration, for super-hydrophobic compounds such as DB[a,l]P, sorption to the glass vessels can be significant, whereby eq 1 would have resulted in erroneous n_{MNP} values. To circumvent this, the amount of DB[a,l]P on LDPE_84 and PA-6_42 was determined by dissolving the loaded MNPs in hot xylenes (70 °C) and formic acid, respectively, followed by quantification of the released DB[a,l]P by GC-MS (see Section S2 for details). The results are presented in Table 1. The B[a]P loadings of selected polymers determined with this method confirm the values obtained with the other two approaches.

2.3. Sequential Digestion of PAH-Sorbed MNPs in GI Fluid Simulants. The in vitro digestion procedure in saliva, gastric, small and large intestine fluid simulants was based on the *Deutsches Institut fur Normung* (DIN) 19738 standard[45] and a previous publication,[46] but modified for the digestion of PAH-loaded MNPs rather than soil or nanoparticles. Importantly, the incubation times in different fluid simulants (5 min in artificial saliva, 2 h in gastric, 4 h in small intestinal and 18 h in large intestinal fluid simulants) represent average digestion times in the human GIT, and therefore are considered to reflect realistic desorption conditions, as opposed to equilibration conditions relevant for characterizing desorption in different environmental compartments. Of note, the volumes of the fluid simulants applied for artificial digestion (i.e., 40 mL for the gastric phase, 40 mL for the small intestinal phase) are comparable to the average GI liquid volumes of fasted humans.[76] Increased volumes as a result of food and beverage intake as well as lower particle concentrations may shift relative desorption rates to higher values.

100 mL Duran glass vials and PAH-loaded MNPs in the mass range of 25−75 mg were used in the in vitro digestion experiments as specified below. The fluid simulant (Section S3, Table S3) for each GI phase was freshly prepared for every experiment, and the pH was adjusted with 1 M HCl or NaOH to the values shown in Figure 1, using a Knick 765 Calimatic pH meter (Berlin, Germany). In vitro digestions were performed by incubating samples in a Burgwedel shaker

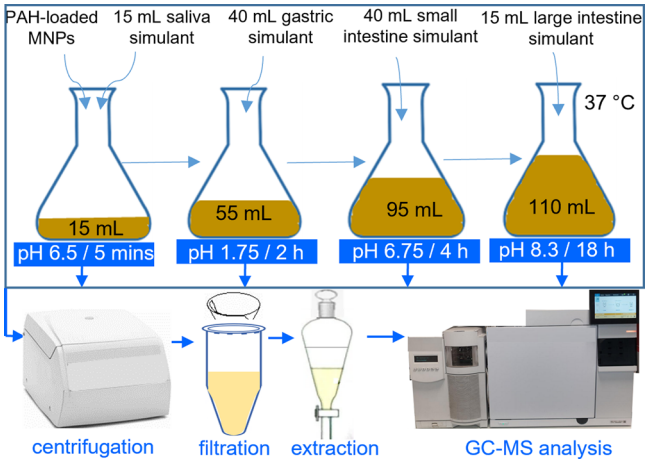

Figure 1. Workflow for the in vitro digestion of PAH-sorbed MNPs. Each digestive phase was either analyzed for the amount of desorbed PAH (↓) or transferred to the next stage (→) for sequential digestion.

https://doi.org/10.1021/acsomega.3c09380
ACS Omega 2024, 9, 24281−24290

(Gesellschaft für Labortechnik GmbH, Germany) operated at 250 rpm and positioned inside an incubation chamber (Binder GmbH, Tuttlingen, Germany) operated at 37 °C. All digested samples were centrifuged using a 1S-R centrifuge (Thermo-Fisher Scientific, Germany) and filtered using 0.7 μm Whatman GF/F glass microfiber filters.

In vitro digestion in artificial saliva was performed by transferring 15 mL of saliva fluid simulant to the digestion vial and adjusting the pH to 6.5 ± 0.1. To start the digestion procedure, a specific amount (25−75 mg) of PAH-loaded MNPs was added to the vial, followed by 5 min incubation. For gastric phase digestion, 40 mL gastric fluid simulant was subsequently added to the mixture, and the pH was adjusted to 1.75 ± 0.1, followed by 2 h incubation. For small intestine phase digestion, 40 mL small intestine fluid simulant were subsequently added to the mixture, the pH was adjusted to 6.5 ± 0.1 and samples were incubated for 4 h. Finally, digestion in the large intestine phase was assessed by adding 15 mL large intestine fluid simulant to the resulting mixture, the pH was adjusted to 8.3 ± 0.1, followed by 18 h incubation. Likewise, the untreated MNPs (without prior loading with PAHs) also underwent sequential digestion as described above and the resulting fluid simulants were analyzed for their PAH contents as negative controls.

For each digestive phase, the desorbed PAHs were analyzed by subjecting the samples to 15 min of centrifugation, followed by filtration and the addition of internal standard to the filtrates. 1000 ng of B[*a*]P-d_{12} and DB[*a,i*]P were used as internal standards for B[*a*]P and DB[*a,l*]P, respectively, while 500 ng of Anth-d_{10} were used for experiments involving Anth. To extract the desorbed PAHs, the filtrates were transferred into a 250 mL separatory funnel and extracted with 2 × 5 and 2 × 25 mL hexane for saliva and gastric fluid simulant filtrates, respectively. Small and large intestinal phase filtrates were extracted using 2 × 30 mL hexane. For calibration, different concentrations of the target PAHs were spiked into control samples consisting of GI fluid simulants without PAH-loaded MNPs. The calibration mixtures and samples were incubated and processed identically. The resulting matrix- and method-matched calibrations (Figure S3, Table S4) were performed sequentially for each GI phase. The hexane extracts were concentrated to <1 mL in a Buchi R-215 Rotavapor system (Flawil, Switzerland) and analyzed by GC-MS. The cumulative relative desorption (CRD) of the PAHs in each GI phase was calculated according to eq 3, where n_{des} is the amount of PAH desorbed in the fluid simulant.

$$CRD(\%) = \frac{n_{des}(\text{ng})}{n_{MNP}(\text{ng})} \times 100(\%) \quad (3)$$

2.4. Data Analysis. GC-MS data were processed with MassHunter software (Agilent, versions B.06.00 and B.05.00). Microsoft Excel 2016 was used for additional data processing. Two-tailed *t* test analysis of the data was performed with GraphPad Prism 9 (GraphPad Software, USA).

3. RESULTS AND DISCUSSION

We aimed to investigate the desorption of PAHs from 11 different MNPs (Table S1, Figures S1/S2). Initially, the MNPs were loaded with PAHs to yield environmentally relevant sorbate concentrations[44] (Table 1, ∼44−95 ng/mg). The PAH-loaded MNPs were then sequentially digested in different GI fluid simulants as schematically depicted in Figure 1. Thereafter, the digested mixtures were separated from MNPs by centrifugation and filtration, and the resulting filtrates containing the released PAHs were quantified via online-coupled GC-MS using matrix and method-matched calibrations (Figure S3, Table S4). From the obtained data we finally assessed the potential human exposure to PAHs through the ingestion of contaminated MNPs.

3.1. Desorption of Benzo[*a*]pyrene from MNPs during Sequential Digestion in Gastrointestinal Fluid Simulants. We initially determined to which extent desorption of PAHs from MNPs would occur in the different compartments of the GIT. To this end, we utilized B[*a*]P as a representative PAH and examined the desorption from three different MNPs (PA-6_42, TPU_est_arom and LDPE_84) in specific GI fluid simulants (see Table S3 for compositions) applying incubation times that correspond to typical retention times during digestion.

The desorbed amount of B[*a*]P in the saliva simulant after 5 min of incubation was below the limit of detection (LOD, see Table S4) and was therefore considered negligible for the three studied MNPs. An increase in the cumulative relative desorption (CRD, the sum of the released amount of PAH during sequential digestion relative to the sorbed amount on the MNPs) along the gastric and both intestinal fluid simulants was observed in the order of LDPE_84 < TPU_est_arom < PA-6_42 (Figure 2a).

Specifically, the CRD for B[*a*]P ranged from 4.0 ± 1.1% to 15.0 ± 3.5% for the three MNPs after 2 h incubation in the gastric fluid simulant. A further 2.6 ± 1.7% to 9.8% ± 1.7% of B[*a*]P desorbed upon transfer of the gastric chyme into the small intestine fluid simulant and incubating the mixture for 4 h, resulting in CRDs of 13.8 ± 2.8% to 19.0 ± 1.8%. Lastly, when the mixture was transferred to the large intestine fluid simulant and digested for 18 h, an additional 4.9 ± 0.6% to 10.3 ± 4.1% of B[*a*]P desorbed from the MNPs. This resulted in CRD values of 20.9% ± 1.3% to 29.3 ± 5.9% along the four tested fluids simulating the passage through the whole digestive tract (Figure 2a).

It has been suggested that proteins and enzymes present in the gastric fluid simulant enhance the solubility of hydrophobic compounds.[47−50] As depicted in Figure 2b, mucin, bovine serum albumin (BSA) and pepsin indeed facilitated the release of hydrophobic B[*a*]P from PA-6_42 MNPs in this medium. Specifically, a release of 8 ± 1% of the loaded B[*a*]P was observed in the gastric fluid simulant in the absence of pepsin, which increased to 17 ± 1% and 20 ± 5% when a physiologically relevant pepsin concentration of 1.4 mg/mL or a 3-fold higher concentration (4.2 mg/mL) was applied (Figure S4). In addition, amphipathic bile acids in the small intestine fluid simulants have been reported to promote the solubilization of hydrophobic organic compounds, including B[*a*]P,[47,51,52] which may explain the observed relatively high CRDs for this compartment. These results suggest that the desorption of organic compounds from MNPs is dependent on the GI fluid composition and the concentrations of individual constituents. This underscores the need for a standardized method to investigate the in vitro digestion of MNPs in order to ensure data comparability.

Absorption of nutrients occurs mainly in the small intestine, while in the large intestine, indigestible food components are further processed by bacteria of the microbiome.[53] Across the three MNPs, approximately 5 to 10% of the total amount of desorbed B[*a*]P were released into the large intestine fluid

https://doi.org/10.1021/acsomega.3c09380
ACS Omega 2024, 9, 24281−24290

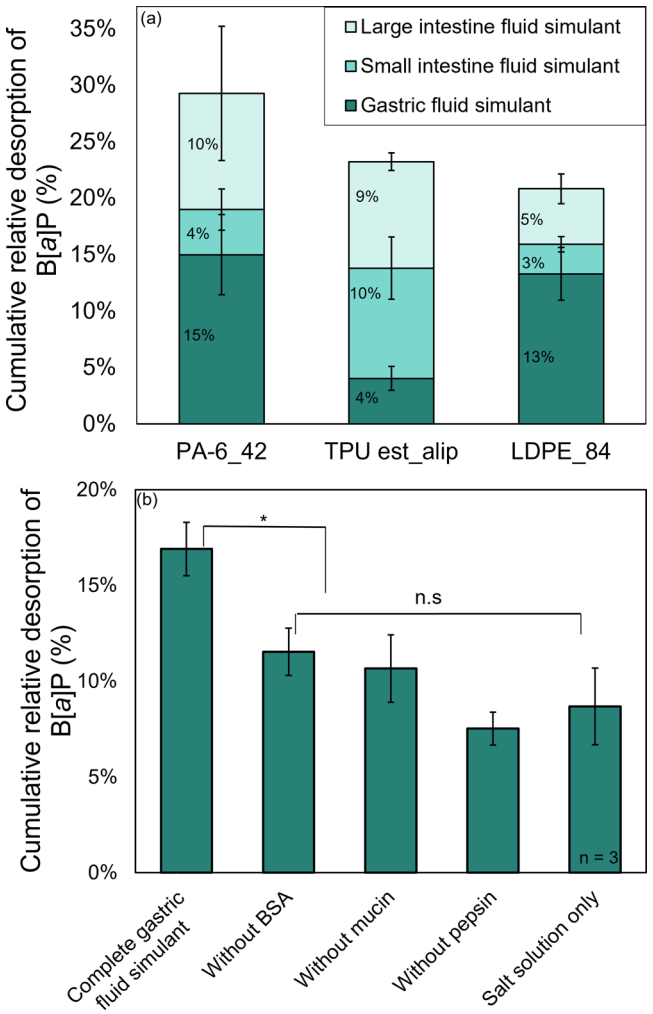

Figure 2. (a): Cumulative relative desorption (CRD) of microplastics-sorbed B[*a*]P during sequential in vitro digestion in different human GI fluid simulants (n = 3, mean ± SD). (b): Effect of gastric fluid simulant components on the CRD of B[*a*]P from PA-6_42 MNPs (n = 2, mean ± SD, * significantly different (p < 0.05), n.s. = not significant at *).

simulant (Figure 2a). Thus, the contribution to the overall CRD is comparable to that observed in the previous two fluids despite the much longer in vitro digestion time (18 h) in relation to gastric (2 h) and small intestine (4 h) fluid simulants. The rate of desorption is presumably slowed down in the large intestinal fluid simulant after an initial rather rapid desorption in the gastric/small intestine fluid simulants.[54,55] In total, the CRD for B[*a*]P did not exceed ∼30% across the three investigated MNPs.

3.2. Comparison of the Cumulative Relative Desorption of B[*a*]P from Eleven Different MNPs in the Small Intestine Fluid Simulant. Digestion and absorption of ingested food and nutrients predominantly occurs in the stomach and small intestine.[53] We therefore decided to compare 11 selected MNP variants for their cumulative desorption of B[*a*]P during sequential digestion up to the small intestine fluid simulant (Figure 3).

The CRD values for most of the MNPs were rather moderate, typically ranging from 4% (PU_arom_1C) to 19% (PA-6_42). Only PA-6_7 showed an exceptionally high CRD

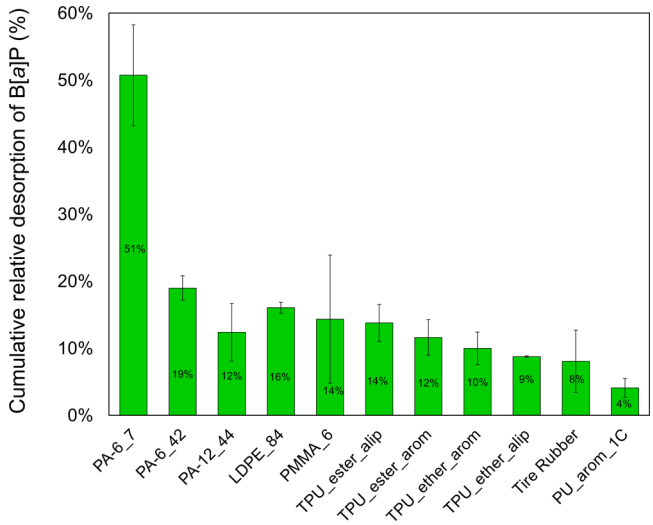

Figure 3. Comparison of the cumulative relative desorption (CRD) of microplastics-sorbed B[*a*]P during sequential digestion up to the small intestine fluid simulant (containing the preceding saliva and gastric fluid simulants). Each experiment was performed at least in triplicate (n = 3, mean ± SD). The CRD values of PA-6_42, LDPE_84, and TPU_est_alip are replotted from Figure 2a.

(51%). This could be related to reversible water absorption by PA-6 materials.[56−58] Hydration may result in increased chain segment mobility, thus significantly lowering the glass transition temperature and stiffness of this polymer.[59,60] This could facilitate diffusion-driven transport of dissolved B[*a*]P from the bulk matrix of the polymer to the aqueous medium. Bulk sorption of estradiol sorbates to PA-6 powders was indeed recently demonstrated by Hummel et al.[61]

The overall comparable CRD values can be explained by the non-equilibrium conditions during in vitro digestion. The cumulative release of B[*a*]P from MNPs in the small intestine fluid simulant was determined after a total incubation time of ca. 6 h. Previous studies demonstrated that equilibrium times for the desorption of POPs from microplastics in GI fluid simulants are in the order of weeks to years.[54,55] Therefore, unlike for sorption under quasi-equilibrium conditions, where B[*a*]P distribution coefficients for the same MNPs differed by over 100-fold,[36] the desorption of B[*a*]P within typical time frames for digestion in humans differed only by 10-fold.

The sorption mechanism presumably also has an influence on the desorption rate. Apart from PMMA_6 and PU_arom_1C, all other MNPs are derived from rubbery polymers, where partitioning of B[*a*]P molecules into the bulk of the particles, in addition to surface adsorption, is considered to significantly contribute to the overall B[*a*]P load.[36] Indeed, the cross-linked PU_1C_arom MNPs desorbed the least B[*a*]P (Figure 3), possibly due to restricted B[*a*]P diffusion through the bulk polymer network.[54]

Particle size and surface area seem to have an influence on the CRD, but other factors such as the chemical nature of the polymers might be more important. Specifically, PA-6_7 and PMMA_6 have similar size distributions (Section S1, Figure S2) but the CRD of B[*a*]P from PA-6_7 was 3.5-fold higher than from PMMA_6. When comparing the same polymer type in two different size ranges, we found that the B[*a*]P release was enhanced by 2.7-fold for the smaller-sized PA-6_7 particles compared to PA-6_42. However, this can be only partially explained by the larger surface area to volume

https://doi.org/10.1021/acsomega.3c09380
ACS Omega 2024, 9, 24281−24290

ratio.[25,62,63] The specific surface area, determined by the Brunauer−Emmett−Teller (BET) method, is 6-fold higher for PA-6_7 (2.16 m^2/g) compared to PA-6_42 (0.37 m^2/g). These examples point to diffusion from the bulk of the MNP particles also playing a role in the desorption process.

To investigate the influence of polymer aging on desorption, PA-6 and TPU MNPs were photoaged via UV-light exposure for 1000 or 2000 h, respectively, and subsequently loaded with B[*a*]P. In contrast to sorption which was studied under quasi-equilibrium conditions in water,[36] photoaging had a negligible effect on the CRD of B[*a*]P in the small intestine fluid simulant (Figure S5). Interestingly, Fourier-transform infrared (FTIR) spectroscopy of the aged and nonaged MNPs indicated an increase in the carbonyl, hydroxyl and amine functional group content on the MNP surfaces (Section S5, Figure S6). This implies that increased surface functionalization of the aged rubbery MNPs had no significant effect on desorption, further suggesting that diffusion from the bulk of these polymers is rate-limiting for desorption.

Considering the various influences of polymer type as well as morphology, including pore volumes,[38] and of the compositions of the different GI fluid simulants on the desorption process, it can be inferred that the release of PAHs from MNPs in the GIT is a complex phenomenon. Further research is needed to fully elucidate how individual factors specifically modulate desorption of different POPs from MNPs.

3.3. Comparison of the Desorption of Different PAHs from MNPs. To ascertain the cumulative relative desorption of PAHs other than B[*a*]P from MNPs in the small intestine fluid simulant, PA and LDPE particles were chosen as examples, as these polymer classes showed the highest sorption[36] and desorption of B[*a*]P (Figure 3). PA-6_42 and LDPE_84 MNPs were loaded individually with Anth and DB[*a,l*]P. The PAHs differ in their physicochemical properties (Table S2) and sorption behaviors.[36] As shown in Figure 4a,

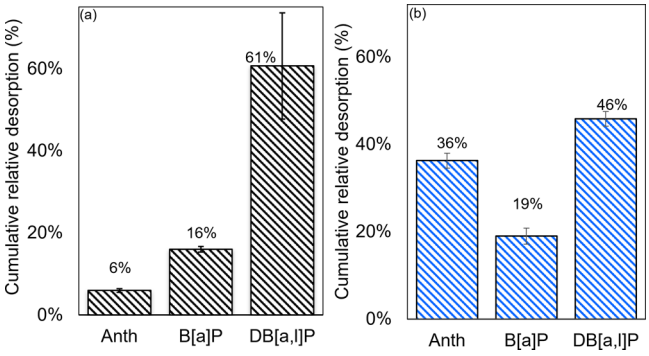

Figure 4. Cumulative relative desorption of PAHs from (a): LDPE_84, (b): PA-6_42 during sequential digestion up to the small intestine fluid simulant (containing the preceding saliva and gastric fluid simulants). Each experiment was performed at least in duplicate ($n \geq 2$, mean ± SD).

the CRD of PAHs sorbed to LDPE_84 differed by over an order of magnitude and increased according to Anth (6 ± 1%) < B[*a*]P (16 ± 1%) < DB[*a,l*]P (61 ± 13%), while for PA-6_42, CRDs of 36 ± 2% (Anth), 19 ± 2% (B[*a*]P), and 46 ± 2% (DB[*a,l*]P) were quantified (Figure 4b).

Sorption of organic pollutants, including PAHs, to sorbents such as LDPE and PA-6 can principally occur via both surface adsorption[64,65] and absorption into the bulk.[61,66] Depending on the specific contribution of each sorption mode, the relative concentrations of the PAHs at the surface versus the bulk will differ. In the case of DB[*a,l*]P in this study, surface adsorption rather than bulk absorption may have dominated the sorption process given its larger molar volume and very low water solubility compared to Anth and B[*a*]P (Table S2). This would explain the observed rapid and comparable desorption of DB[*a,l*]P from the surfaces of LDPE_84 and PA-6_42 MNPs, which also have similar surface areas of 0.33 m^2/g and 0.37 m^2/g, respectively.[36]

For LDPE, B[*a*]P and particularly Anth are increasingly distributed to the bulk due to their decreasing molar volumes and thus enhanced diffusion during loading of the MNPs. Within the limited time frame of the desorption experiment, the release of Anth is therefore slowest since diffusion to the particle/water interface is restricted.

Surprisingly, in the case of PA-6, a higher degree of desorption was observed for Anth compared to B[*a*]P. This behavior can be explained by the dynamics of (de)sorption in PA-6 materials compared to LDPE. PA-6 is a polymer well-known for its high-water absorption capacity.[56−58] We hypothesize that due to the higher water solubility of Anth, this PAH is better solubilized from the bulk of the PA-6 MNPs during swelling with the GI fluid simulants, thereby facilitating its transport into the bulk of the liquid phase.

Analysis of both the small and large intestine fluid simulants following sequential digestion of six selected pristine MNP variants (without prior loading with PAHs) indicated that none of the three investigated PAHs were released (Section S6 and Figure S7). However, for Tire Rubber particles, pyrene was detected in both fluid simulants. It is noteworthy that Tire Rubber is the only polymer investigated in this study that has been exposed to the environment for extended periods. All other MNPs are therefore unlikely to have accumulated POPs including PAHs.[27,67]

4. ASSESSMENT OF THE CONTRIBUTION OF MICROPLASTICS TO TOTAL HUMAN DIETARY PAH EXPOSURE

Understanding the contribution of MNPs as carriers of POPs such as PAHs is vital to assessing the potential health risk posed by human exposure to MNPs. Released PAHs could become translocated across the GI barriers via the gut epithelial cells, among other pathways,[23,68] and might become distributed across the body or accumulate in specific tissues.[19] To provide some insights into the contribution of microplastics to the overall human PAH intake, we estimated the maximum daily intake *MDI* of PAHs from MNPs with eq 4.[23,69]

$$MDI(\mu g/kg\ bw) = \frac{C_{PAH}(\mu g/g) \times M_{ingest}(g) \times Bioac_{SI}(\%)}{BW(kg\ bw)} \quad (4)$$

Regarding the concentration of PAHs sorbed to MNPs, C_{PAH}, the values shown in Table 1 were utilized, which represent the equilibrium sorption achieved in our previous study with realistic aqueous PAH concentrations in the ng/L range.[36] Notably, the resulting PAH loads (44−95 $\mu g/g$) are within the range of total PAH concentrations (3.4−120 $\mu g/g$) quantified from MNPs collected from the environment.[44] For the mass of ingested MNPs, M_{ingest}, a real-life scenario estimate of 4.1 × 10^{-6} g/capita/day[70] was used. This was calculated as the 97.5th percentile of MNP intake from air, eight widely

https://doi.org/10.1021/acsomega.3c09380
ACS Omega 2024, 9, 24281−24290

consumed food types, two widely consumed fruits and four popular vegetables[70] (see Section S7 for a detailed analysis). $Bioac_{SI}$ is the bioaccessible fraction of PAHs released from MNPs into the small intestine, where absorption of nutrients but also of contaminants predominantly takes place. This corresponds to the experimentally determined cumulative PAH release in the small intestine fluid simulant (also containing the preceding saliva and gastric fluid simulants, see Figure 3 for B[*a*]P and Figure 4 for Anth and DB[*a*,*l*]P). Previous assessments of the contribution of MNPs to human chemical exposure either assumed 100% bioaccessibility of sorbed chemicals[23,40] or utilized probabilistically modeled values.[70] We applied an average body weight *BW* of 70 kg in our exposure assessment.

As depicted in Table 2, the estimated MDI values of the three PAHs from the different MNP variants investigated in this study range from 0.2−2.4 pg/kg bw/day. These results allowed to estimate the individual contributions to the total human dietary PAH intake TI_{cont} (%) according to eq 5,

$$TI_{cont}(\%) = \frac{MDI(\text{pg/kg bw/day})}{TI(\text{pg/capita/day})} \times BW(\text{kg bw}) \times 100(\%) \quad (5)$$

where *TI* is the median dietary intake of PAHs by European adults.[71] *TI* values of 0.34, 0.17, and 0.63 μg/capita/day[71] were utilized for Anth, B[*a*]P, and DB[*a*,*l*]P, respectively (see Section S7 for details).

As shown in Table 2, the estimated relative contribution of MNPs as PAH carriers to the total dietary PAH exposure under realistic scenarios is very small, with the highest contribution estimated at 0.1% for PA-6_7. However, uncertainties remain especially related to the magnitude of MNP exposure, which could become significant at local hotspots.[72,73] Here, environmental MNP concentrations can be several orders of magnitude higher than the general estimate.[74] Although it is unclear to what extent this elevates the MNP uptake via food consumption and inhalation, the contribution of MNPs as carriers of ubiquitous PAHs could be significantly augmented if the exposure scenario involves a local source of PAH pollution. Depending on the assumed MNP uptake[75] and PAH loadings, the calculated contribution of MNPs as carriers of PAHs can increase to values far exceeding the estimated human PAH uptake. Nevertheless, based on the currently available knowledge on microplastic ingestion, our study suggests that this contribution is very small (∼0.1%).

Table 2. Estimated Maximum Daily Human Intake (*MDI*) of PAHs from Ingested PAH-Contaminated MNPs and Contributions to the Total Daily Dietary PAH Exposure (TI_{cont})

PAH	MNPs	estimated maximum daily human PAH intake (*MDI*) from ingested MNPs (pg/kg bw/day)	contribution of MNP intake to total daily human dietary PAH exposure (TI_{cont})
B[*a*]P	PA-6_7	2.36	0.10%
	PA-6_42	0.87	0.04%
	PA-12	0.57	0.02%
	LDPE_84	0.74	0.03%
	PMMA_7	0.51	0.02%
	TPU est_alip	0.63	0.03%
	TPU est arom	0.53	0.02%
	TPU eth_arom	0.46	0.02%
	TPU eth_alip	0.40	0.02%
	Tire Rubber	0.37	0.02%
	PU_binder 1C	0.17	0.01%
DB[*a*,*l*]P	PA-6_42	1.40	0.02%
	LDPE_84	1.85	0.02%
Anth	PA-6_42	0.92	0.02%
	LDPE_84	0.17	<0.01%

5. CONCLUSIONS

In this study, the desorption of PAHs from a variety of polydisperse MNP variants, including photoaged materials, was investigated via a physiology-based sequential in vitro digestion model based on the DIN 19738 standard. Using environmentally relevant loadings of B[*a*]P as a representative PAH, a cumulative release in the range of 21−29% was observed for three different MNPs (PA-6_42, TPU_est_arom and LDPE_84) after sequential passage through all four investigated fluid simulants. This emphasizes that the release of these toxicologically relevant POPs from microplastic particles upon ingestion can indeed occur to a significant extent.

When comparing the desorption of B[*a*]P from 11 different microplastic materials up to the small intestinal phase, ten of them showed moderate CRDs in the range of 4−19%, with PA-6_7 being an exception (CRD: 51%). Presumably, the high-water absorption capacity of this polymer facilitated enhanced transport of bulk-bound B[*a*]P to the particle surface. Photoaging of MNPs composed of TPU or PA-6 had no significant effect on desorption, despite chemical alteration of the polymer surfaces being observed via FTIR-spectroscopy. This further highlights the predominant contribution of bulk desorption of B[*a*]P for these particles.

In addition to B[*a*]P, the sequential desorption of Anth and DB[*a*,*l*]P into the small intestinal fluid simulant was studied for PA-6 and LDPE MNPs. The degree of desorption varied based on both the type of PAH and the MNP material employed. DB[*a*,*l*]P, for example, exhibited the strongest desorption from both MNPs, presumably resulting from its predominant adsorption to the particle surfaces. B[*a*]P and Anth showed less but varying desorption, possibly due to different modes of transport from the bulk to the particle surface for the two polymers.

Finally, we estimated the contribution of MNPs as PAH carriers to the total human dietary PAH exposure to be very small (≤0.1%). Future studies will therefore investigate the leaching of chemical additives and non-intentionally added substances from real-life MNPs in human gastrointestinal fluid simulants.

■ ASSOCIATED CONTENT

Supporting Information

The Supporting Information is available free of charge at https://pubs.acs.org/doi/10.1021/acsomega.3c09380.

Size distribution of MNPs investigated in this study (Table S1); Selected physicochemical properties of PAH sorbates used in this study (Table S2); Scanning

https://doi.org/10.1021/acsomega.3c09380
ACS Omega 2024, 9, 24281−24290

electron microscopy (SEM) and particle size characterization (Section S1); Analysis of PAH concentrations in MNPs (Section S2); Preparation of the gastrointestinal fluid simulants (Section S3); Quantification of PAHs via GC-MS (Section S4); Characterization of selected MNPs by Fourier-transform infrared (FTIR) spectroscopy (Section S5); Quality control and release of PAHs from unloaded MNPs (Section S6); Estimates of the daily intakes of MNPs and PAHs (Section S7) (PDF)

AUTHOR INFORMATION

Corresponding Authors

Andrea Haase − *Department of Chemical and Product Safety, German Federal Institute for Risk Assessment, 10589 Berlin, Germany*; Email: andrea.haase@bfr.bund.de

Alexander Roloff − *Department of Chemical and Product Safety, German Federal Institute for Risk Assessment, 10589 Berlin, Germany*; orcid.org/0000-0003-1886-3288; Email: alexander.roloff@bfr.bund.de

Authors

Emeka Ephraim Emecheta − *Department of Chemical and Product Safety, German Federal Institute for Risk Assessment, 10589 Berlin, Germany; Bayreuth Center for Ecology and Environmental Research (BayCEER), University of Bayreuth, 95448 Bayreuth, Germany*; orcid.org/0009-0001-9558-7603

Patrizia Marie Pfohl − *BASF SE, 67056 Ludwigshafen, Germany*; orcid.org/0000-0002-1580-8833

Wendel Wohlleben − *BASF SE, 67056 Ludwigshafen, Germany*; orcid.org/0000-0003-2094-3260

Complete contact information is available at: https://pubs.acs.org/10.1021/acsomega.3c09380

Author Contributions

AR and AH conceptualized the study. EEE (FTIR, PAH loading, in vitro digestion, data analysis) and PMP (SEM, particle size) performed the experiments for this study. EEE and AR wrote the manuscript with contributions from AH, WW, and PP. AR and AH supervised the study. All authors read and approved the final manuscript.

Funding

This work was funded by the BMBF (German Federal Ministry of Education and Research) project entitled InnoMat.Life − Innovative Materials and new production processes: Safety along the Life Cycle and in industrial value chains, with funding numbers 03XP0216A (BfR) and 03XP0216X (BASF).

Notes

The authors declare no competing financial interest.

ACKNOWLEDGMENTS

This study was supported by the German Federal Institute for Risk Assessment (BfR). We thank Klaudia Michna for her dedicated technical assistance with the GC-MS instrument.

ABBREVIATIONS

Anth:anthracene
B[*a*]P:benzo[*a*]pyrene
BET:Brunauer−Emmett−Teller
CRD:cumulative relative desorption
DB[*a,l*]P:dibenzo[*a,l*]pyrene
DIN:Deutsches Institut für Normung
FAO:Food and Agriculture Organization of the United Nations
FTIR:Fourier-transform infrared
GIT:gastrointestinal tract
GI:gastrointestinal
GC-MS:gas chromatography−mass spectrometry
HCl:hydrochloric acid
LOD:limit of detection
LDPE:low-density polyethylene
MDI:maximum daily intake
MNP:micro- and nanoplastics
PA:polyamide
PAH:polycyclic aromatic hydrocarbon
POP:persistent organic pollutant
PMMA:poly(methyl methacrylate)
WHO:World Health Organization
NaOH:sodium hydroxide
UV:ultraviolet
SD:standard deviation
SEM:scanning electron microscopy
T_g:glass transition temperature
TI:total intake
TPU:thermoplastic polyurethane

REFERENCES

(1) Lim, X. Microplastics are everywhere - but are they harmful? *Nature* **2021**, *593* (7857), 22−25.

(2) Ageel, H. K.; Harrad, S.; Abdallah, M. A. Occurrence, human exposure, and risk of microplastics in the indoor environment. *Environ. Sci. Process Impacts* **2022**, *24* (1), 17−31.

(3) Lebreton, L.; Andrady, A. Future scenarios of global plastic waste generation and disposal. *Palgrave Communications* **2019**, *5* (1), 6.

(4) Cox, K. D.; Covernton, G. A.; Davies, H. L.; Dower, J. F.; Juanes, F.; Dudas, S. E. Human Consumption of Microplastics. *Environ. Sci. Technol.* **2019**, *53* (12), 7068−7074.

(5) Koelmans, A. A.; Mohamed Nor, N. H.; Hermsen, E.; Kooi, M.; Mintenig, S. M.; De France, J. Microplastics in freshwaters and drinking water: Critical review and assessment of data quality. *Water Res.* **2019**, *155*, 410−422.

(6) Oliveri Conti, G.; Ferrante, M.; Banni, M.; Favara, C.; Nicolosi, I.; Cristaldi, A.; Fiore, M.; Zuccarello, P. Micro- and nano-plastics in edible fruit and vegetables. The first diet risks assessment for the general population. *Environ. Res.* **2020**, *187*, No. 109677.

(7) Kutralam-Muniasamy, G.; Perez-Guevara, F.; Elizalde-Martinez, I.; Shruti, V.C. Branded milks - Are they immune from microplastics contamination? *Sci. Total Environ.* **2020**, *714*, No. 136823.

(8) Shruti, V.C.; Perez-Guevara, F.; Elizalde-Martinez, I.; Kutralam-Muniasamy, G. First study of its kind on the microplastic contamination of soft drinks, cold tea and energy drinks - Future research and environmental considerations. *Sci. Total Environ.* **2020**, *726*, No. 138580.

(9) Li, Y.; Peng, L.; Fu, J.; Dai, X.; Wang, G. A microscopic survey on microplastics in beverages: the case of beer, mineral water and tea. *Analyst* **2022**, *147* (6), 1099−1105.

(10) Karami, A.; Golieskardi, A.; Keong Choo, C.; Larat, V.; Galloway, T. S.; Salamatinia, B. The presence of microplastics in commercial salts from different countries. *Sci. Rep* **2017**, *7*, 46173.

(11) Makhdoumi, P.; Hossini, H.; Pirsaheb, M. A review of microplastic pollution in commercial fish for human consumption. *Rev. Environ. Health* **2023**, *38*, 97.

(12) Schwabl, P.; Köppel, S.; Königshofer, P.; Bucsics, T.; Trauner, M.; Reiberger, T.; Liebmann, B. Detection of Various Microplastics in Human Stool: A Prospective Case Series. *Ann. Int. Med.* **2019**, *171* (7), 453−457.

(13) Luqman, A.; Nugrahapraja, H.; Wahyuono, R. A.; Islami, I.; Haekal, M. H.; Fardiansyah, Y.; Putri, B. Q.; Amalludin, F. I.; Rofiqa, E. A.; Götz, F.; Wibowo, A. T. Microplastic Contamination in Human Stools, Foods, and Drinking Water Associated with Indonesian Coastal Population. *Environments* **2021**, *8* (12), 138.
(14) Gossmann, I.; Sussmuth, R.; Scholz-Bottcher, B. M. Plastic in the air?! - Spider webs as spatial and temporal mirror for microplastics including tire wear particles in urban air. *Sci. Total Environ.* **2022**, *832*, No. 155008.
(15) Dris, R.; Gasperi, J.; Mirande, C.; Mandin, C.; Guerrouache, M.; Langlois, V.; Tassin, B. A first overview of textile fibers, including microplastics, in indoor and outdoor environments. *Environ. Pollut.* **2017**, *221*, 453−458.
(16) Amato-Lourenço, L. F.; Carvalho-Oliveira, R.; Júnior, G. R.; Dos Santos Galvão, L.; Ando, R. A.; Mauad, T. Presence of airborne microplastics in human lung tissue. *J. Hazard Mater.* **2021**, *416*, No. 126124.
(17) Vianello, A.; Jensen, R. L.; Liu, L.; Vollertsen, J. Simulating human exposure to indoor airborne microplastics using a Breathing Thermal Manikin. *Sci. Rep* **2019**, *9* (1), 8670.
(18) Gasperi, J.; Wright, S. L.; Dris, R.; Collard, F.; Mandin, C.; Guerrouache, M.; Langlois, V.; Kelly, F. J.; Tassin, B. Microplastics in air: Are we breathing it in? *Current Opinion in Environmental Science & Health* **2018**, *1*, 1−5.
(19) Wright, S. L.; Kelly, F. J. Plastic and Human Health: A Micro Issue? *Environ. Sci. Technol.* **2017**, *51* (12), 6634−6647.
(20) Catarino, A. I.; Macchia, V.; Sanderson, W. G.; Thompson, R. C.; Henry, T. B. Low levels of microplastics (MP) in wild mussels indicate that MP ingestion by humans is minimal compared to exposure via household fibres fallout during a meal. *Environ. Pollut.* **2018**, *237*, 675−684.
(21) *Dietary and inhalation exposure to nano- and microplastic particles and potential implications for human health*; WHO: Geneva, 2022.
(22) Lehner, R.; Weder, C.; Petri-Fink, A.; Rothen-Rutishauser, B. Emergence of Nanoplastic in the Environment and Possible Impact on Human Health. *Environ. Sci. Technol.* **2019**, *53* (4), 1748−1765.
(23) *Microplastics in fisheries and aquaculture. Status of knowledge on their occurrence and implications for aquatic organisms and food safety*; Food Agriculture Organization (FAO), 2017.
(24) Rostami, I.; Juhasz, A. L. Assessment of Persistent Organic Pollutant (POP) Bioavailability and Bioaccessibility for Human Health Exposure Assessment: A Critical Review. *Critical Reviews in Environmental Science and Technology* **2011**, *41* (7), 623−656.
(25) Teuten, E. L.; et al. Transport and release of chemicals from plastics to the environment and to wildlife. *Philos. Trans R Soc. Lond B Biol. Sci.* **2009**, *364* (1526), 2027−45.
(26) Chen, C.-F.; Ju, Y.-R.; Lim, Y. C.; Hsu, N.-H.; Lu, K.-T.; Hsieh, S.-L.; Dong, C.-D.; Chen, C.-W. Microplastics and their affiliated PAHs in the sea surface connected to the southwest coast of Taiwan. *Chemosphere* **2020**, *254*, No. 126818.
(27) Rochman, Chelsea M.; Hoh, Eunha; Hentschel, Brian T.; Kaye, Shawn Long-term field measurement of sorption of organic contaminants to five types of plastic pellets: implications for plastic marine debris. *Environ. Sci. Technol.* **2013**, *47* (3), 1646−54.
(28) Tan, X.; Yu, X.; Cai, L.; Wang, J.; Peng, J. Microplastics and associated PAHs in surface water from the Feilaixia Reservoir in the Beijiang River, China. *Chemosphere* **2019**, *221*, 834−840.
(29) Varjani, S. J.; Gnansounou, E.; Pandey, A. Comprehensive review on toxicity of persistent organic pollutants from petroleum refinery waste and their degradation by microorganisms. *Chemosphere* **2017**, *188*, 280−291.
(30) Corsini, E.; Luebke, R. W.; Germolec, D. R.; DeWitt, J. C. Perfluorinated compounds: emerging POPs with potential immunotoxicity. *Toxicol. Lett.* **2014**, *230* (2), 263−70.
(31) Kumar, M.; Sarma, D. K.; Shubham, S.; Kumawat, M.; Verma, V.; Prakash, A.; Tiwari, R. Environmental Endocrine-Disrupting Chemical Exposure: Role in Non-Communicable Diseases. *Front Public Health* **2020**, *8*, No. 553850.
(32) Bang, S.-Y.; Ha, Y.; Kwon, J.-H. Relative Importance of Microplastics as Vectors of Hydrophobic Organic Chemicals to Marine Fish and Seabirds. *Ocean Science Journal* **2021**, *56* (4), 355−363.
(33) Bakir, A.; Rowland, S. J.; Thompson, R. C. Enhanced desorption of persistent organic pollutants from microplastics under simulated physiological conditions. *Environ. Pollut.* **2014**, *185*, 16−23.
(34) Koelmans, A. A.; Bakir, A.; Burton, G. A.; Janssen, C. R. Microplastic as a Vector for Chemicals in the Aquatic Environment: Critical Review and Model-Supported Reinterpretation of Empirical Studies. *Environ. Sci. Technol.* **2016**, *50* (7), 3315−26.
(35) Guo, H.; Zheng, X.; Ru, S.; Luo, X.; Mai, B. The leaching of additive-derived flame retardants (FRs) from plastics in avian digestive fluids: The significant risk of highly lipophilic FRs. *J. Environ. Sci. (China)* **2019**, *85*, 200−207.
(36) Emecheta, E. E.; Borda, D. B.; Pfohl, P. M.; Wohlleben, W.; Hutzler, C.; Haase, A.; Roloff, A. A comparative investigation of the sorption of polycyclic aromatic hydrocarbons to various polydisperse micro- and nanoplastics using a novel third-phase partition method. *Microplastics and Nanoplastics* **2022**, *2* (1), 29.
(37) Ziccardi, L. M.; et al. Microplastics as vectors for bioaccumulation of hydrophobic organic chemicals in the marine environment: A state-of-the-science review. *Environ. Toxicol. Chem.* **2016**, *35* (7), 1667−76.
(38) Liu, X.; Gharasoo, M.; Shi, Y.; Sigmund, G.; Huffer, T.; Duan, L.; Wang, Y.; Ji, R.; Hofmann, T.; Chen, W. Key Physicochemical Properties Dictating Gastrointestinal Bioaccessibility of Microplastics-Associated Organic Xenobiotics: Insights from a Deep Learning Approach. *Environ. Sci. Technol.* **2020**, *54* (19), 12051−12062.
(39) Hu, X.; Yu, Q.; Gatheru Waigi, M.; Ling, W.; Qin, C.; Wang, J.; Gao, Y. Microplastics-sorbed phenanthrene and its derivatives are highly bioaccessible and may induce human cancer risks. *Environ. Int.* **2022**, *168*, No. 107459.
(40) *Microplastics in drinking-water*; World Health Organization, 2019.
(41) Pfohl, P.; Roth, C.; Meyer, L.; Heinemeyer, U.; Gruendling, T.; Lang, C.; Nestle, N.; Hofmann, T.; Wohlleben, W.; Jessl, S. Microplastic extraction protocols can impact the polymer structure. *Microplastics and Nanoplastics* **2021**, *1* (1), 8.
(42) Pfohl, P.; Bahl, D.; Rückel, M.; Wagner, M.; Meyer, L.; Bolduan, P.; Battagliarin, G.; Hüffer, T.; Zumstein, M.; Hofmann, T.; Wohlleben, W. Effect of Polymer Properties on the Biodegradation of Polyurethane Microplastics. *Environ. Sci. Technol.* **2022**, *56* (23), 16873−16884.
(43) Pfohl, P.; Wagner, M.; Meyer, L.; Domercq, P.; Praetorius, A.; Hüffer, T.; Hofmann, T.; Wohlleben, W. Environmental Degradation of Microplastics: How to Measure Fragmentation Rates to Secondary Micro- and Nanoplastic Fragments and Dissociation into Dissolved Organics. *Environ. Sci. Technol.* **2022**, *56* (16), 11323−11334.
(44) Mai, L.; Bao, L.-J.; Shi, L.; Liu, L.-Y.; Zeng, E. Y. Polycyclic aromatic hydrocarbons affiliated with microplastics in surface waters of Bohai and Huanghai Seas, China. *Environ. Pollut.* **2018**, *241*, 834−840.
(45) *Soil quality - Bioaccessibility of organic and inorganic pollutants from contaminated soil material*, DIN 19738; Deutsches Institut fur Normung E.V.,2017,
(46) Yu, Y. Q.; Yang, J. Y. Oral bioaccessibility and health risk assessment of vanadium(IV) and vanadium(V) in a vanadium titanomagnetite mining region by a whole digestive system in-vitro method (WDSM). *Chemosphere* **2019**, *215*, 294−304.
(47) Zhang, Y.; Pignatello, J. J.; Tao, S.; Xing, B. Bioaccessibility of PAHs in Fuel Soot Assessed by an in Vitro Digestive Model with Absorptive Sink: Effect of Food Ingestion. *Environ. Sci. Technol.* **2015**, *49* (24), 14641−8.
(48) Wu, J.; Lu, J.; Wu, J. Effect of gastric fluid on adsorption and desorption of endocrine disrupting chemicals on microplastics. *Frontiers of Environmental Science & Engineering* **2022**, *16* (8), 104.
(49) Tao, S.; Li, L.; Ding, J.; Zhong, J.; Zhang, D.; Lu, Y.; Yang, Y.; Wang, X.; Li, X.; Cao, J.; Lu, X.; Liu, W. Mobilization of soil-bound

https://doi.org/10.1021/acsomega.3c09380
ACS Omega 2024, 9, 24281−24290

residue of organochlorine pesticides and polycyclic aromatic hydrocarbons in an in vitro gastrointestinal model. *Environ. Sci. Technol.* **2011**, *45* (3), 1127−32.
(50) Oomen, A. G.; Sips, A. J. A. M.; Groten, J. P.; Sijm, D. T. H. M.; Tolls, J. Mobilization of PCBs and lindane from soil during in vitro digestion and their distribution among bile salt micelles and proteins of human digestive fluid and the soil. *Environ. Sci. Technol.* **2000**, *34* (2), 297−303.
(51) Ahrens, M. J.; Hertz, J.; Lamoureux, E. M.; Lopez, G. R.; McElroy, A. E.; Brownawell, B. J. The role of digestive surfactants in determining bioavailability of sediment-bound hydrophobic organic contaminants to 2 deposit-feeding polychaetes. *Mar. Ecol.: Prog. Ser.* **2001**, *212*, 145−157.
(52) Masset, T.; Ferrari, B. J. D.; Dudefoi, W.; Schirmer, K.; Bergmann, A.; Vermeirssen, E.; Grandjean, D.; Harris, L. C.; Breider, F. Bioaccessibility of Organic Compounds Associated with Tire Particles Using a Fish In Vitro Digestive Model: Solubilization Kinetics and Effects of Food Coingestion. *Environ. Sci. Technol.* **2022**, *56* (22), 15607−15616.
(53) Fonseca, M. R. J. *An Engineering Understanding of the Small Intestine*. Ph.D. Thesis, School of Chemical Engineering, The University of Birmingham, 2011.
(54) Mohamed Nor, N. H.; Koelmans, A. A. Transfer of PCBs from Microplastics under Simulated Gut Fluid Conditions Is Biphasic and Reversible. *Environ. Sci. Technol.* **2019**, *53* (4), 1874−1883.
(55) Liu, P.; Wu, X.; Liu, H.; Wang, H.; Lu, K.; Gao, S. Desorption of pharmaceuticals from pristine and aged polystyrene microplastics under simulated gastrointestinal conditions. *J. Hazard Mater.* **2020**, *392*, No. 122346.
(56) Sambale, A. K.; Stanko, M; Emde, J.; Stommel, M. Characterisation and FE Modelling of the Sorption and Swelling Behaviour of Polyamide 6 in Water. *Polymers (Basel)* **2021**, *13* (9), 1480.
(57) Puffr, R.; Šebenda, J. On the Structure and Properties of Polyamides. XXVII. The Mechanism of Water Sorption in Polyamides. *Journal of Polymer Science Part C: Polymer Symposia* **1967**, *16* (1), 79−93.
(58) Monson, L.; Braunwarth, M.; Extrand, C. W. Moisture absorption by various polyamides and their associated dimensional changes. *J. Appl. Polym. Sci.* **2008**, *107* (1), 355−363.
(59) Reimschuessel, H. K. Relationships on the effect of water on glass transition temperature and young's modulus of nylon 6. *Journal of Polymer Science: Polymer Chemistry Edition* **1978**, *16* (6), 1229−1236.
(60) Dlubek, G.; Redmann, F.; Krause-Rehberg, R. Humidity-induced plasticization and antiplasticization of polyamide 6: A positron lifetime study of the local free volume. *J. Appl. Polym. Sci.* **2002**, *84* (2), 244−255.
(61) Hummel, Darius; Fath, Andreas; Hofmann, Thilo; Hüffer, Thorsten Additives and polymer composition influence the interaction of microplastics with xenobiotics. *Environmental Chemistry* **2021**, *18* (3), 101.
(62) Rochman, C. M. The Complex Mixture, Fate and Toxicity of Chemicals Associated with Plastic Debris in the Marine Environment. In *Marine Anthropogenic Litter*; Bergmann, M., Gutow, L., Klages, M., Eds.; Springer, 2015; pp 117−140.
(63) Jang, M.; et al. Styrofoam Debris as a Source of Hazardous Additives for Marine Organisms. *Environ. Sci. Technol.* **2016**, *50* (10), 4951−60.
(64) Fu, L.; Li, J.; Wang, G.; Luan, Y.; Dai, W. Adsorption behavior of organic pollutants on microplastics. *Ecotoxicol Environ. Safety* **2021**, *217*, No. 112207.
(65) Satshi Endo, A. K., Sorption of Hydrophobic Organic Compounds to Plastics in the Marine Environment: Equilibrium. In *Hazardous Chemicals Associated with Plastics in the Marine Environment*; Takada, H., Karapanagioti, H. K., Eds.; Springer International Publishing: Switzerland, 2016.
(66) Huffer, T.; Hofmann, T. Sorption of non-polar organic compounds by micro-sized plastic particles in aqueous solution. *Environ. Pollut.* **2016**, *214*, 194−201.
(67) Coffin, S.; Dudley, S.; Taylor, A.; Wolf, D.; Wang, J.; Lee, I.; Schlenk, D. Comparisons of analytical chemistry and biological activities of extracts from North Pacific gyre plastics with UV-treated and untreated plastics using in vitro and in vivo models. *Environ. Int.* **2018**, *121* (Pt 1), 942−954.
(68) Powell, J. J.; Faria, N.; Thomas-McKay, E.; Pele, L. C. Origin and fate of dietary nanoparticles and microparticles in the gastrointestinal tract. *J. Autoimmun* **2010**, *34* (3), J226−33.
(69) *Presence of microplastics and nanoplastics in food, with particular focus on seafood*. EFSA, 2016.
(70) Mohamed Nor, N. H.; Kooi, M.; Diepens, N. J.; Koelmans, A. A. Lifetime Accumulation of Microplastic in Children and Adults. *Environ. Sci. Technol.* **2021**, *55* (8), 5084−5096.
(71) *Polycyclic Aromatic Hydrocarbons − Occurrence in foods, dietary exposure and health effects*; European commision health and consumer protection, 2002.
(72) Norén, F. *Small plastic particles in Coastal Swedish waters*; KIMO: Sweden, 2007.
(73) Chai, B.; Wei, Q.; She, Y.; Lu, G.; Dang, Z.; Yin, H. Soil microplastic pollution in an e-waste dismantling zone of China. *Waste Manag* **2020**, *118*, 291−301.
(74) Hartmann, N. B; Rist, S.; Bodin, J.; Jensen, L. H.; Schmidt, S. N; Mayer, P.; Meibom, A.; Baun, A. Microplastics as vectors for environmental contaminants: Exploring sorption, desorption, and transfer to biota. *Integr Environ. Assess Manag* **2017**, *13* (3), 488−493.
(75) Senathirajah, K.; Attwood, S.; Bhagwat, G.; Carbery, M.; Wilson, S.; Palanisami, T. Estimation of the mass of microplastics ingested - A pivotal first step towards human health risk assessment. *J. Hazard Mater.* **2021**, *404* (Pt B), No. 124004.
(76) Mudie, D. M.; Murray, K.; Hoad, C. L.; Pritchard, S. E.; Garnett, M. C.; Amidon, G. L.; Gowland, P. A.; Spiller, R. C.; Amidon, G. E.; Marciani, L. Quantification of gastrointestinal liquid volumes and distribution following a 240 mL dose of water in the fasted state. *Mol. Pharmaceutics* **2014**, *11* (9), 3039−47.

https://doi.org/10.1021/acsomega.3c09380
ACS Omega 2024, 9, 24281−24290